Sensors and Materials, Vol. 37, No. 3 (2025) 861–881
MYU Tokyo

S & M 3962

Efficient Direction of Arrival Estimation Using Particle Swarm Optimization for Hybrid Analog and Digital Massive Multiple-input Multiple-output Receiving Array

Tsui-Ping Chang[1*] and Chao-Li Meng[2**]

[1]Department of Computer Science and Information Engineering, National Taichung University of Science and Technology, Taichung 404, Taiwan, ROC
[2]IoT Research Center, Feng Chia University, Taichung 407, Taiwan, ROC

(Received October 23, 2024; accepted February 26, 2025)

Keywords: massive MIMO, hybrid analog and digital signal processing, direction-of-arrival estimation, phase alignment, particle swarm optimization, quantum-behaved particle swarm optimization

In this paper, we address the challenges of achieving both low complexity and high resolution in direction-of-arrival (DOA) sensing of signals impinging on an antenna sensor array. We propose a phase alignment (PA) method enhanced with particle swarm optimization (PSO) algorithms for hybrid analog and digital (HAD) massive multiple-input multiple-output (MIMO) receiving arrays. This approach aims to reduce costs and improve energy efficiency while supporting high network access capability and meeting the demands of massive internet of things (mIoT). These methods include linear search techniques such as traditional analog PA, HADPA, and hybrid digital and analog PA. The objective is to estimate the DOA of signals from multiple sources. It has been demonstrated that the search complexity and estimation accuracy of the PA methods are contingent upon the number of search grids employed during the peak searching process, which is time-consuming, and the required number of search grids is not readily discernible. Furthermore, PSO algorithms can be employed to address these issues in the context of DOA estimation. Additionally, the quantum-behaved PSO (QPSO) does not require velocity vectors, results in a reduction in the number of parameters, and is simpler to implement. We also present a DOA search method based on QPSO, which is designed to reduce further the computational complexity. Finally, several computer simulation results are provided for illustrative and comparative purposes.

1. Introduction

The fifth-generation (5G) mobile communication system promotes the development of internet of things (IoT), and its objective is to enhance system capacity to accommodate growing data demands. The core performance characteristics of 5G directly meet the needs of massive IoT (mIoT) systems with an enormous number of IoT devices, including low power consumption, large-scale connectivity, high speed, and low latency.(1) The third-generation partnership project

*Corresponding author: e-mail: applechang@nutc.edu.tw
**Corresponding author: e-mail: clmeng74@gmail.com
https://doi.org/10.18494/SAM5408

ISSN 0914-4935
https://myukk.org/

(3GPP) posits that should a 5G base station achieve the same coverage extent as the Long-term Evolution (LTE) system under identical transmitting power, the energy loss will increase exponentially owing to the adoption of the high-frequency band transmission. Consequently, the deployment of the massive multiple-input multiple-output (MIMO) system, beamforming and tracking techniques, and other related technologies becomes indispensable. The MIMO system consists of a large antenna array with more than a hundred elements, significantly more than the number of antenna elements used in the MIMO technique of the 4G LTE physical layer. This allows the system to achieve a high degree of freedom. As the number of antenna sensors increases, the beam width is expected to become smaller, which will result in an increase in the direction-of-arrival (DOA) estimation error of signals' impinging direction sensing. Regarding the design of beamformers in the context of massive MIMO systems, the deployment of all-digital beamforming technology is perceived as one of the most significant design challenges, owing to the substantial hardware cost and power consumption associated with a single receiver unit. In traditional massive MIMO systems, each antenna is connected to a radio frequency (RF) chain, which results in significant increases in hardware cost, complexity, and power consumption.[2] In the context of a business application, the number of antenna elements tends to be on a massive scale, which consequently leads to increases in the computing load of the beamformer, the complexity of the electric circuit, and the cost of the digital construct. Achieving DOA estimation with high computational efficiency, high resolution, and robust performance in a hybrid analog and digital (HAD) massive MIMO antenna array is both significant and challenging.[2]

Precise DOA sensing in an antenna sensor array for mIoT ensures highly efficient network access. However, a fully digital antenna sensor array in massive MIMO systems incurs high hardware cost and complexity. In recent years, the problem of DOA estimation for analog and hybrid beamforming techniques has attracted the attention of numerous researchers. Analog beamforming (AB) is a technique that concentrates energy by adjusting the coefficient of the antenna board at the RF terminal. Hybrid beamforming is a technique that combines the advantages of analog and digital methods. It divides the antenna array into many blocks and uses a set of digital-to-analog converters (DACs) and analog-to-digital converters (ADCs) in the same block. The configuration of an appropriate antenna array allows for the reduction in the number of converters, thus reducing hardware cost. Furthermore, the implementation of HAD beamforming enables the acquisition of considerable antenna gain.[3] The objective of a previous study[4] is to eliminate interfering signals in the analog domain, thereby minimizing the required ADC analysis. For a given analysis capability, Islam proposed an optimal analog beamformer to minimize the estimated mean square error between the intended user and other recipients.[4] There is only one emission source that has been considered in the literature[5] for the presented simplified design of a DOA estimation method, root-MUSIC-HDAPA or HDAPA, and its simplified derivation of the Cramer–Rao lower bound (CRLB). Consequently, the discussion of the DOA estimation under this HAD structure is limited to a single signal source.

The use of massive MIMO as a receiving array results in a significant enhancement of the accuracy of DOA estimation owing to the array's ultrahigh resolution. Consequently, it is imperative to devise a high-resolution direction-finding methodology for the massive MIMO

system. Most of the research on the DOA estimation problem of massive MIMO systems currently focuses on all-digital beamforming technology. Some methods have been proposed in the literature, including the minimum variance distortionless response (MVDR)[6] and multiple signal classification (MUSIC)[7] methods. For systems employing massive MIMO, these methods entail a significant computational complexity, primarily owing to the vast dimensions of the autocorrelation matrix of the array input signal. In any case, these methods must implement a linear search algorithm on the spatial spectrum to estimate the DOA. However, the accuracy of the estimation depends on the step size of the searching grid, which will result in high computational complexity.

To address the computational demands of the search process, heuristic evolutionary algorithms have been incorporated into the research domain of DOA estimation in recent years. The development of these algorithms is based on the observed natural phenomena, and the inspiration obtained from much phenomena serves as the theoretical basis of the algorithms. In nature, numerous species of organisms engage in collective behavior, establishing social systems for the purposes of food acquisition, migration, and group organization. These social systems are composed of simple individuals and their groups, which engage in interactive behaviors. A growing number of scientists are investigating the compositional structure, information communication, and behavioral patterns of biological social systems, including ant foraging and nesting, the collective movements of birds and fish, and the gravitational force between particle masses. Swarm intelligence is defined as intelligence derived from a multitude of individuals on the basis of self-organizing group behavior.[8] Particle swarm optimization (PSO)[9] is a stochastic global optimization algorithm that simulates the social behavior of bird flocks. PSO is a relatively straightforward algorithm to implement and is computationally efficient owing to its low memory and CPU requirements. It can solve both linear and nonlinear optimization problems. PSO is a commonly used technique in the design of antenna arrays, as evidenced by the numerous reports in the literature.[9,10] To reduce the computational load associated with searching, Meng *et al.*[11] applied PSO to DOA estimation, replacing the traditional spectrum search with the use of the MUSIC algorithm. Hung[12] proposed a memetic PSO (MPSO) algorithm combined with a noise variance estimator. The MPSO incorporates the re-estimation of the noise variance and iterated local search algorithms into the PSO algorithm, resulting in a higher efficiency and a reduction in the level of a nonuniform noise effect under a low signal-to-noise ratio (SNR).

The search trajectory of the traditional PSO algorithm[13] is based on the particles' own experience and that of the swarm. This results in the algorithm converging to the optimal solution. Consequently, the particles adhere to the original trajectory and gradually attain the convergence state, resulting in the search space of each iteration of the particle being unable to encompass the entire feasible space throughout the search process. Consequently, the accuracy of local searches is not optimal, and the convergence rate will decline as the search progresses. To enhance the optimal searching ability and convergence speed of particles in the feasible area, it is necessary to overcome the shortcomings of the traditional PSO algorithm. Quantum concepts can be integrated into the PSO algorithm.[14–17] In quantum-behaved PSO (QPSO), each particle exhibits quantum behavior during the search process. Consequently, only the

particle's position vector and a control parameter are considered, which results in a higher convergence speed and an enhanced optimization ability. The QPSO algorithm represents a developed version of the PSO algorithm that does not require a velocity vector, has fewer parameters, and is easier to implement. In the literature, the DOA search of multiple signal sources, that is, the multi-objective optimization problem, is treated as a single-objective optimization problem to effectively reduce the probability of missed signal detection. Subsequently, the QPSO is employed to determine an optimal signal subspace by minimizing the orthogonality error, thereby enabling DOA determination.

In this paper, we address the problem of low-complexity and high-resolution DOA estimation based on phase alignment (PA) methods with PSO algorithms for HAD massive MIMO receiving arrays. Our research works deal with the electromagnetic wave signals' impinging direction sensing and receiving from antenna sensors. In this paper, we discuss the DOA sensing of impinging signals in mIoT networks using PA methods, PSO-based estimators, and QPSO-based estimators for achieving cost reduction and high resolution. For the DOA sensing of impinging signals, we employ heuristic PSO-based algorithms to address the nondeterministic polynomial (NP) problem of peak searches in the uncertain search grid of the antenna sensor array in mIoT. This approach enhances the capability to maintain high network accessiblity. It has been demonstrated that the search complexity and estimation accuracy of the PA methods are contingent upon the number of search grids employed during the peak searching process, which is time-consuming, and the required number of search grids is not readily discernible. First, three PA methods utilizing conventional spectrum searching, namely, traditional analog PA (APA), HADPA, and hybrid digital and analog PA (HDAPA), are replaced by standard PSO searching for multiple signal sources. Furthermore, PSO algorithms can be employed to address these issues in the context of DOA estimation. Additionally, the QPSO does not require velocity vectors, results in a reduction in the number of parameters, and is simpler to implement. In addition, we present a QPSO-based estimator that utilizes the average best particle position of the population as a guiding principle for the search of the swarm. This approach has the potential to enhance the accuracy of DOA estimation and prevent premature convergence. Furthermore, several computer simulation results are provided for illustrative and comparative purposes.

2. Background Knowledge

2.1 Signal model

Consider an architecture comprising N antenna elements connected to an HAD beamformer at the receiver, as illustrated in Fig. 1. This architecture has been employed to reduce the cost of hardware and energy consumption, although it has the consequence of reducing performance. In this architecture, the receiver is responsible for equipping N omnidirectional antennas, which are subsequently divided into K sub-antenna arrays. Each sub-antenna array comprises M antenna elements ($N = KM$), with the number of RF chains N_{RF} being smaller than that of antenna elements ($N_{RF} \leq N$). The antenna elements are followed by phase shifters that feed the RF chains, and each subset of antenna array elements is connected to only one RF chain. As

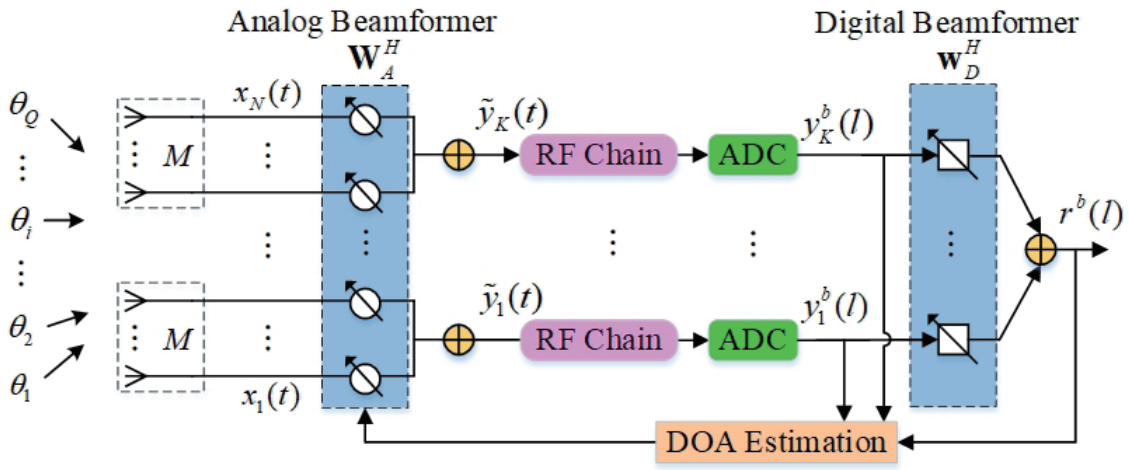

Fig. 1. (Color online) HAD beamforming architecture at the receiver.[5]

depicted in Fig. 1, HAD receives signals $s_i(t)e^{j2\pi f_c t}$ with different arrival direction angles θ_i. The received signal from N antenna elements is presented as the vector $\boldsymbol{y}(t)=[y_1(t),y_2(t),\cdots,y_N(t)]^T$, and the received signal from the nth antenna element can be written as

$$y_n(t) = \sum_{i=1}^{Q} s_i(t)e^{j2\pi f_c\left(t-\left(\tau_i-\frac{(n-1)d}{c}\sin\theta_i\right)\right)} + v(t), n=1,2,\cdots,N, \tag{1}$$

where $d=0.5\lambda$ is the spacing between adjacent antenna array elements and c is the speed of light. Suppose the reference point is the first element of the antenna array and τ_i is the propagation delay of the ith signal transmitter to the reference point. $v(t)$ is additive white Gaussian noise with zero means and the covariance value σ_v^2.

Considering AB, the output $\tilde{y}_k^b$ of the kth subarray can be represented as

$$\tilde{y}_k(t)=\sum_{i=1}^{Q}\sum_{m=1}^{M} s_i(t)e^{j\left(2\pi f_c t-2\pi f_c\tau_{k,m,i}-\alpha_{k,m,i}\right)}+v_k(t), k=1,2,\cdots,K, \tag{2}$$

where $\alpha_{k,m,i}$ is the analog beam formation/PA of the ith signal source to the phase corresponding to the mth antenna of the kth subarray. τ_0 is the propagation delay from the transmitter to the reference point, the first element of the antenna array of the receiver. $\tau_{k,m,i}$ is the propagation delay of the ith received signal at the mth antenna element of the kth subarray aligned to the DOA θ_i and can be represented as

$$\tau_{k,m,i}=\tau_0-\frac{\left((k-1)M+m-1\right)}{c}\sin\theta_i, I=1,2,\cdots,Q. \tag{3}$$

All K output signals of subarrays formulated using Eq. (2) can be stacked as $\tilde{\boldsymbol{y}}(t) \in \mathbb{C}^{K\times 1}$ and expressed as

$$\tilde{\boldsymbol{y}}(t) = e^{j2\pi f_c t}\boldsymbol{W}_A^H \boldsymbol{A}(\theta)\boldsymbol{s}(t) + \boldsymbol{v}(t), \tag{4}$$

where the signal vector $\boldsymbol{s}(t) = [s_1(t), s_2(t), \cdots, s_Q(t)]^T$ and $\boldsymbol{v}(t) = [v_1(t), v_2(t), \cdots, v_K(t)]^T$ is an additive white Gaussian noise vector. The $N \times Q$ dimensional steering matrix $\boldsymbol{A}(\theta) = [\boldsymbol{a}(\theta_1), \boldsymbol{a}(\theta_2), \cdots, \boldsymbol{a}(\theta_Q)]$ and the steering vector $\boldsymbol{a}(\theta) = [1, e^{j\frac{2\pi}{\lambda}d\sin\theta}, \cdots, e^{j\frac{2\pi}{\lambda}(N-1)d\sin\theta}]^T$. The AB matrix $\boldsymbol{W_A}$ is the $N \times K$ dimensional block diagonal matrix of phase shifting and is represented as

$$\boldsymbol{W}_A = \begin{bmatrix} \boldsymbol{w}_{A,1} & \boldsymbol{0} & \cdots & \boldsymbol{0} \\ \boldsymbol{0} & \boldsymbol{w}_{A,2} & \cdots & \boldsymbol{0} \\ \vdots & \vdots & \ddots & \vdots \\ \boldsymbol{0} & \boldsymbol{0} & \cdots & \boldsymbol{w}_{A,K} \end{bmatrix}, \tag{5}$$

where $\boldsymbol{w}_{A,k} = \frac{1}{\sqrt{M}}[e^{j\alpha_{k,1}}, e^{j\alpha_{k,2}}, \cdots, e^{j\alpha_{k,M}}]^T$ is the AB vector of subarray k. After passing through the K parallel RF chains of the analog beamformer, the output signal $\tilde{\boldsymbol{y}}(t)$ [Eq. (4)] is down-converted to the baseband signal vector and given by

$$\boldsymbol{y}(t) = \boldsymbol{W}_A^H \boldsymbol{A}(\theta)\boldsymbol{s}(t) + \boldsymbol{v}(t). \tag{6}$$

Then, the baseband signal vector goes through the ADC and output,

$$\boldsymbol{y}^b(l) = \boldsymbol{W}_A^H \boldsymbol{A}(\theta)\boldsymbol{s}(l) + \boldsymbol{v}^b(l), \tag{7}$$

where b is the index of the temporal block, each block is constituted by L data samples, and L is the number of data sampling processes of each block. Finally, passing through the operation by the digital beamformer (DB) w_D, the signal vector [Eq. (7)] becomes

$$r^b(l) = \boldsymbol{w}_D^H \boldsymbol{W}_A^H \boldsymbol{A}(\theta)\boldsymbol{s}(l) + \boldsymbol{w}_D^H \boldsymbol{v}^b(l), \tag{8}$$

where the DB vector $\boldsymbol{w}_D = [w_{D,1}, w_{D,2}, \cdots, w_{D,K}]^T$.

2.2 Traditional APA DOA estimator

Suppose the emmision direction of the signal source is $\{\theta_i\}_{i=1}^{Q}$ as depicted in Fig. 1. After passing through the AB and ADC, the summation of the output signal of the kth subarray can be obtained and represented as

$$\begin{aligned} y_k^b(l) &= \sum_{i=1}^{Q} \boldsymbol{w}_{A,k}^H \boldsymbol{a}_k(\theta_i) s_i(l) + v_k^b(l) \\ &= \tfrac{1}{\sqrt{M}} \sum_{i=1}^{Q} s_i(l) e^{j\frac{2\pi}{\lambda}(k-1)Md\sin\theta_i} \sum_{m=1}^{M} e^{j\left(\frac{2\pi}{\lambda}(m-1)d\sin\theta_i - \alpha_{k,m}\right)} + v_k^b(l), \end{aligned} \tag{9}$$

where $\boldsymbol{a}_k(\theta_i) = [e^{j\frac{2\pi}{\lambda}(k-1)Md\sin\theta_i}, e^{j\frac{2\pi}{\lambda}(k-2)Md\sin\theta_i}, \cdots, e^{j\frac{2\pi}{\lambda}(kM-1)d\sin\theta_i}]^T$ is the steering vector of the ith signal source impinging on the kth subarray and λ is the signal wavelength. Because only the APA has been used, the DB vector $\boldsymbol{w_D}$ has been fixed as a vector with a value of 1, that is, $\boldsymbol{w_D}$ = [1, 1, …, 1]. After that, we will maximize the output power of the received signal $r(l)$ by optimizing the vector $\boldsymbol{w_{A,k}}$ as demonstrated in Fig. 1. First, we define the average output power of HAD as

$$P^b = \tfrac{1}{L} \sum_{l=1}^{L} [r^b(l) r^b(l)^*] = \tfrac{1}{L} \boldsymbol{r}^b \boldsymbol{r}^{bH} \ , \tag{10}$$

where $\boldsymbol{r}^b = [r^b(1), \cdots, r^b(L)]$, $r^b(l) = \sum_{k=1}^{K} y_k^b(l)$, and l = 1, 2, …, L. Then, Eq. (10) can be expanded as

$$\begin{aligned} P_r^b(\theta) &= \tfrac{1}{LN^2} \sum_{n=1}^{L} [r^b(l) r^b(l)^H] \\ &= \tfrac{1}{LN^2} \sum_{l=1}^{L} \{ [\sum_{k=1}^{K} [\tfrac{1}{\sqrt{M}} \sum_{i=1}^{Q} s_i(l) e^{j\frac{2\pi}{\lambda}(k-1)Md\sin\theta_i} \sum_{m=1}^{M} e^{j(\frac{2\pi}{\lambda}(m-1)d\sin\theta_i - \alpha_{k,m})}] + \sum_{k=1}^{K} v_k^b(l)] \\ &\quad \times [\sum_{k=1}^{K} [\tfrac{1}{\sqrt{M}} \sum_{i=1}^{Q} s_i(l) e^{j\frac{2\pi}{\lambda}(k-1)Md\sin\theta_i} \sum_{m=1}^{M} e^{j(\frac{2\pi}{\lambda}(m-1)d\sin\theta_i - \alpha_{k,m})}] + \sum_{k=1}^{K} v_k^b(l)]^H \}, \end{aligned} \tag{11}$$

where

$$\alpha_{k,m} = \frac{2\pi}{\lambda}\big((k-1)M + (m-1)\big) d\sin\theta \, . \tag{12}$$

By adjusting and varying the θ of Eq. (12), we can optimize the receiving power [Eq. (11)], and the maximum values will be allocated on the direction angles $\{\theta_1, \theta_2, \ldots, \theta_Q\}$. From the observation of [Eq. (11)], suppose the impinging signal direction is θ_i, the optimal AB weight vector $\boldsymbol{w_{A,k}}$ is exactly aligned with the array manifold produced by θ_i under the condition

$$\alpha_{k,m} = \frac{2\pi}{\lambda}\big((k-1)M + (m-1)\big) d\sin\theta_i \, . \tag{13}$$

It forces all the signals of N antenna elements to merge on the output point coherently and provides the maximum output power. For linear searching, dividing the range of direction angle θ into C subsections from $-(\pi/2)$ to $\pi/2$ and defining the phase searching step size as $\Delta\theta = \pi/C$, when the searching angle θ varies from $-(\pi/2)$ to $\pi/2$, the setting θ will be chosen from the angle set $\boldsymbol{\Theta} = \{-(\pi/2), -(\pi/2) + \Delta\theta, \ldots, (\pi/2) - \Delta\theta, (\pi/2)\}$. The APA, demonstrated in Fig. 1, in front of ADC is different from the digital PA (DPA) in the sense that the APA cannot preserve the received data. In other words, each grid search should calculate and transfer the new analog alignment phase to the N phase shifter; at the same time, the newly received signal block b will be used to calculate the output result of the new searched point and finally find the max received power via comparison. Clearly, achieving high-resolution estimation requires a fine step size. This implies that some parameter will take on an enormous value, resulting in a massive computational load.

2.3 HADPA DOA estimator

The APA algorithm mentioned above shoulde implement linear searching from $-(\pi/2)$ to $\pi/2$ and calculate N values at the same time, which leads to high computational complexity. In this study, we addressed an issue different from that investigated in Ref. 5, which was about the estimation of DOA from a single signal source. Instead, we considered the estimation of DOA from multiple signals and proposed a hybrid PA (HPA) method with low computational complexity. Initially, we separated the phase $\alpha_{k,m}$ of PA into two parts:

$$\alpha_{k,m} = \alpha_m + \alpha_k, \tag{14}$$

where the first part α_m is the phase of eliminating the mth element of each subarray and the second part α_k is the common phase elimination of the kth subarray. This implies that the PA contains two steps: APA and then DPA.

After APA, the output of subarray k can be expressed as

$$\begin{aligned} y_k^b(l) &= \sum_{i=1}^{Q} \boldsymbol{w}_{A,k}^H \boldsymbol{a}_k(\theta_i) s_i(l) + v_k^b(l) \\ &= \frac{1}{\sqrt{M}} \sum_{i=1}^{Q} s_i(l) \underbrace{e^{j\frac{2\pi}{\lambda}(k-1)Md\sin\theta_i}}_{\substack{\text{The common factor} \\ \text{of } k\text{th subarray}}} \sum_{m=1}^{M} e^{j\left(\frac{2\pi}{\lambda}(m-1)d\sin\theta_i - \alpha_m\right)} + v_k^b(l), \end{aligned} \tag{15}$$

where

$$\alpha_k = \frac{2\pi}{\lambda}(k-1)Md\sin\theta\,. \tag{16}$$

For eliminating the common factor of subarray k, the DPA vector can be designed as

$$\boldsymbol{w}_D = [e^{j\alpha_1}, e^{j\alpha_2}, \cdots, e^{j\alpha_K}]^H , \tag{17}$$

where

$$\alpha_k = \frac{2\pi}{\lambda}(k-1)Md\sin\theta . \tag{18}$$

Therefore, in Fig. 1, $r^b(l) = \sum_{k=1}^{K} e^{-j\alpha_k} y_k^b(l)$. As with the derivation of Eq. (11), the average receiving power of the HADPA estimator is presented as

$$\begin{aligned} P_r^b(\theta) &= \frac{1}{LN^2}\sum_{l=1}^{L}[r^b(l)r^b(l)^H] \\ &= \frac{1}{LN^2}\sum_{l=1}^{L}\left\{\left[\frac{1}{\sqrt{M}}\sum_{k=1}^{K}\left[\sum_{i=1}^{Q}s_i(l)e^{j\frac{2\pi}{\lambda}(k-1)Md\sin\theta_i-\alpha_k}\sum_{m=1}^{M}e^{j\left(\frac{2\pi}{\lambda}(m-1)d\sin\theta_i-\alpha_m\right)}\right]\right.\right. \\ &\quad \left.+\sum_{k=1}^{K}e^{-j\alpha_k}v_k^b(l)\right] \\ &\quad \times\left[\frac{1}{\sqrt{M}}\sum_{k=1}^{K}\left[\sum_{i=1}^{Q}s_i(l)e^{j\frac{2\pi}{\lambda}(k-1)Md\sin\theta_i-\alpha_k}\sum_{m=1}^{M}e^{j\left(\frac{2\pi}{\lambda}(m-1)d\sin\theta_i-\alpha_m\right)}\right]\right. \\ &\quad \left.\left.+\sum_{k=1}^{K}e^{-j\alpha_k}v_k^b(l)\right]^H\right\}. \end{aligned} \tag{19}$$

For the signal source $\{\theta_i\}_{i=0}^{Q}$, when $\alpha_k = \frac{2\pi}{\lambda}(k-1)Md\sin\theta_i$ and $\alpha_m = \frac{2\pi}{\lambda}(m-1)d\sin\theta_i$, the max power can be obtained.

2.4 HDAPA DOA estimator

In this section, we present a low-computational-complexity HPA alternative method with a reverse PA order, which encompasses DPA and APA. In the initial phase, the first block of data is employed to perform DPA by linear searching. Once the optimal direction set is identified, a subset of the virtual solutions is incorporated into the set of all M solutions. After that, the following M data blocks are used to perform APA. This implies that the total number of data blocks of PA is $B = M + 1$.

Suppose all the initial phases of the analog shifter are equal to zero, that is, $\boldsymbol{w}_{A,k} = (1/\sqrt{M})[1, 1, ..., 1]^T$, and are substituted to Eq. (9), then the signal of the discrete output sum of the kth subarray of block $b = 1$ is

$$\begin{aligned} y_k^1(l) &= \sum_{i=1}^{Q} \boldsymbol{w}_{A,k}^H \boldsymbol{a}_k(\theta_i) s_i(l) + v_k^1(l) \\ &= \frac{1}{\sqrt{M}}[1,1,\cdots,1] \sum_{i=1}^{Q} \boldsymbol{a}_k(\theta_i) s_i(l) + v_k^1(l) \\ &= \frac{1}{\sqrt{M}} \sum_{i=1}^{Q} [s_i(l) e^{j\frac{2\pi}{\lambda}(k-1)Md\sin\theta_i} g(\theta_i)] + v_k^1(l), \end{aligned} \tag{20}$$

where

$$\begin{aligned} g(\theta_i) &= \sum_{m=1}^{M} e^{j\frac{2\pi}{\lambda}(m-1)d\sin\theta_i} \\ &= \frac{1-e^{j\frac{2\pi}{\lambda}Md\sin\theta_i}}{1-e^{j\frac{2\pi}{\lambda}d\sin\theta_i}}. \end{aligned} \tag{21}$$

$y_k^1(l)$ is set as the input of the DB in Fig. 1, and after passing through DPA, we can obtain

$$\begin{aligned} r^1(l) &= \sum_{k=1}^{K} e^{-j\alpha_k} y_k^1(l) \\ &= \sum_{i=1}^{Q} \left[\frac{1}{\sqrt{M}} g(\theta_i) s_i(l) \sum_{k=1}^{K} e^{j\left(\frac{2\pi}{\lambda}(k-1)Md\sin\theta_i - \alpha_k\right)} \right] + \sum_{k=1}^{K} e^{-j\alpha_k} v_k^1(l) \, . \end{aligned} \tag{22}$$

$r^1(l)$ can be stored in the memory of the receiver; moreover, Eq. (19) can be represented as

$$\begin{aligned} P_r^1(\tilde{\theta}) &= \frac{1}{LN^2} \sum_{l=1}^{L} [r^1(l) r^1(l)^H] \\ &= \frac{1}{LN^2} \sum_{n=1}^{L} \left\{ \left[\sum_{i=1}^{Q} \left(\frac{1}{\sqrt{M}} g(\theta_i) s_i(l) \sum_{k=1}^{K} e^{j\left(\frac{2\pi}{\lambda}(k-1)Md\sin\theta_i - \alpha_k\right)} \right) + \sum_{k=1}^{K} e^{-j\alpha_k} v_k^1(l) \right] \right. \\ &\quad \left. \times \left[\sum_{i=1}^{Q} \left(\frac{1}{\sqrt{M}} g(\theta_i) s_i(l) \sum_{k=1}^{K} e^{j\left(\frac{2\pi}{\lambda}(k-1)Md\sin\theta_i - \alpha_k\right)} \right) + \sum_{k=1}^{K} e^{-j\alpha_k} v_k^1(l) \right]^H \right\}, \end{aligned} \tag{23}$$

where

$$\alpha_k = \frac{2\pi}{\lambda}(k-1)Md\sin\tilde{\theta}_i \, . \tag{24}$$

$\{\tilde{\theta}_i\}_{i=1}^{Q}$ is picking the angle from the angle set $\boldsymbol{\Theta}$. Since it is a DB, the step size can be set as arbitrarily small. If the optimal direction $\{\tilde{\theta}_i\}_{i=1}^{Q}$ has been obtained by performing linear searching to the set $\boldsymbol{\Theta}$, $\{\tilde{\theta}_i\}_{i=1}^{Q}$ apparently satisfies the following approximate identity equation:

$$\frac{2\pi}{\lambda}(k-1)Md\sin\theta_i - \underbrace{\frac{2\pi}{\lambda}(k-1)Md\sin\tilde{\theta}_i}_{\alpha_k} = 2q\pi\,. \tag{25}$$

Here, $k \in S_K = \{0,1,\cdots,K-1\}$ and $q \in S_M = \{0,1,\cdots,M-1\}$. From Eq. (25), for the ith signal source's impinging angle, the feasible solution set $\tilde{\boldsymbol{\Theta}}_i = \{\tilde{\boldsymbol{\theta}}_{i,0}, \tilde{\boldsymbol{\theta}}_{i,1}, \cdots, \tilde{\boldsymbol{\theta}}_{i,M-1}\}$ with the M estimated direction of signal-emitting sources can be obtained. The $\tilde{\boldsymbol{\theta}}_{i,m}$ here represents the impinging angle of the ith signal source in the mth set. The $Q \times M$ dimension matrix $\boldsymbol{A}_m$ can be generated by utilizing the estimated angles of the M sets substituted to Eqs. (16) and (18), that is,

$$\boldsymbol{A}_m = \begin{bmatrix} \alpha_{1,0} & \alpha_{1,0} & \cdots & \alpha_{1,M-1} \\ \alpha_{2,0} & \alpha_{2,1} & \cdots & \alpha_{2,M-1} \\ \vdots & \vdots & \ddots & \vdots \\ \alpha_{Q,0} & \alpha_{Q,1} & \cdots & \alpha_{Q,M-1} \end{bmatrix}. \tag{26}$$

According to Eqs. (16) and (18), $\alpha_{m,j}$ and $\alpha_{k,j}$ correspond to $\tilde{\theta}_{i,m}$,

$$\alpha_{m,j} = \frac{2\pi}{\lambda}(m-1)d\sin\tilde{\theta}_{i,m}\,, \tag{27}$$

and

$$\alpha_{k,j} = \frac{2\pi}{\lambda}(k-1)Md\sin\tilde{\theta}_{i,m}\,. \tag{28}$$

We substitute each row of the above two equations into Eq. (19), and the $P_r^b(\theta)$ of Q signal sources will be generated. In the case of DPA, the sampled and quantized signal can be saved in memory, and only one data block is needed to complete a linear search in the direction angle $[-(\pi/2),\ \pi/2]$ interval. This means that compared with APA, the advantage of DPA is that the delay of DPA and the length of received data are smaller.

The results of the DOA estimation of the spectrum searching estimator in different search grid sizes indicate that the estimation performances of APA, HADPA, and HDAPA estimators are better in smaller search grid sizes. However, this comes at the price of increased computational costs owing to the higher search time consumption associated with smaller search grid selections.

3. PSO-based DOA Estimation

In this study, we started with the examination of the potential for reducing the computational complexity of linear search in the contexts of APA, HADPA, and HDAPA to achieve the objective of reducing the computational complexity. We defined the nonlinear multidimensional maximization fitness function of the swarm intelligence algorithm as[18]

$$fitness = \max_{\theta} \sum_{l=1}^{L} \|\boldsymbol{U}\boldsymbol{U}^{+}\boldsymbol{y}^{b}(l)\|, \tag{29}$$

where $\|\bullet\|$ is the Euclidean norm, $\boldsymbol{U} = [\boldsymbol{W}_1\boldsymbol{w}_{D,1}, \boldsymbol{W}_2\boldsymbol{w}_{D,2}, \cdots, \boldsymbol{W}_Q\boldsymbol{w}_{D,Q}]$ with $\boldsymbol{W}_A = \boldsymbol{W}_1 = \boldsymbol{W}_2 = ... = \boldsymbol{W}_Q$, and $(\bullet)^+$ is a pseudo invariance matrix operation. It is worth noting that the angle estimation of the HDAPA will generate M sets of estimated angles. Therefore, the searches use HADPA as the reference of the initial angle estimation and the search grid is $\mu_1 = 1°$, defining the angle error of each iteration to be within 1° from the previous angle. This eliminates the problem that the angle estimation of the swarm intelligence algorithm falls into the local optimal solution. Given that the initial estimation is a relatively minor component of the overall computational complexity of the swarm intelligence algorithm, it can be considered a negligible factor. Finally, we provide a brief explanation of the search modes of the first three methods as follows:

(1) APA method: searching the θ of $\alpha_{k,m}$ in the $P_r^b(\theta)$ of Eq. (11),
(2) HADPA method: searching the θ of α_k and α_m in the $P_r^b(\theta)$ of Eq. (19), and
(3) HDAPA method: searching the θ of α_k in the $P_r^1(\theta)$ of Eq. (23).

3.1 Standard PSO-based DOA estimator

In this subsection, we introduce the PA methods with the PSO search algorithm for DOA estimation. The PSO algorithm[13] starts from random particles, searches for a better solution than the initial particles, and updates the cluster on the basis of its own experience to find the best solution. PSO starts with a set of randomly generated initial values and then evolves to obtain the best solution. PSO is a one-way message transmission. The entire search process and update are based on the current best-solution mechanism.

In PSO, the solution to each optimization problem is a particle in space. Each particle is a point in Q-dimensional space, and each dimension represents a signal source. First, we assume that the position of the jth particle in the Q-dimensional space is expressed as $\boldsymbol{\theta}_j = [\theta_{j,1}, \theta_{j,2}, \cdots, \theta_{j,Q}]$ and $j = 1, 2, \ldots, N_p$. Before calculating the fitness function, we substitute the estimate $\hat{\theta}_{j,i}^{h}$ corresponding to the ith user into the fitness function for calculation and comparison. Through the dynamic adjustment of uniformly distributed random variables and acceleration, the position change speed of the jth particle is expressed as $\boldsymbol{v}_j = [v_{j,1}, v_{j,2}, \cdots, v_{j,Q}]$. When the particle passes the previous best position, we express it as $\boldsymbol{pbest}_j = [pbest_{j,1}, pbest_{j,2}, ..., pbest_{j,Q}]$. Then, all the particles in PSO have a global best solution in the group, which is $\boldsymbol{gbest}_j = [gbest_{g,1}, gbest_{g,2}, ..., gbest_{g,Q}]$. The particle swarm finds the best position through changes in position and velocity. The jth particle position in the Q-dimensional space at the hth iteration is expressed as $\boldsymbol{\theta}_j^h = [\theta_{j,1}^h, \theta_{j,2}^h, \cdots, \theta_{j,Q}^h]$ and $h = 1, 2, \ldots,$

h_{max}. In the same way, the speed of the jth particle in the Q-dimensional space at the hth iteration is expressed as $\boldsymbol{v}_j^h = [v_{j,1}^h, v_{j,2}^h, \cdots, v_{j,Q}^h]$. Therefore, the update of the speed and position of the jth particle at the (h + 1)th iteration can be expressed as

$$\boldsymbol{v}_j^{h+1} = w^h \boldsymbol{v}_j^h + c_1 \boldsymbol{r}_1^h \times [\boldsymbol{pbest}_j^h + \boldsymbol{\theta}_j^h] + c_2 \boldsymbol{r}_2^h \times [\boldsymbol{gbest}_g - \boldsymbol{\theta}_j^h], \tag{30}$$

$$\boldsymbol{\theta}_j^{h+1} = \boldsymbol{\theta}_j^h + \boldsymbol{v}_j^{h+1}. \tag{31}$$

Note that Eq. (30) can be divided into three parts. The first part $w^h \boldsymbol{v}_j^h$ is the previous inertial velocity of the particle, which can be regarded as the flight experience of the particle. w^h is the inertia weight to maintain the previous motion; here, we assume that the inertia weight linearly decreases from the maximum value w_{max} to the minimum value w_{min}. Generally, w^h is defined to implement a linear decrease in the range between 0.9 and 0.4;[13] then, the inertia weight can be represented as

$$w^h = (w_{max} - w_{min}) \times \frac{(h_{max} - 1) - (h - 1)}{(h_{max} - 1)} + w_{min}. \tag{32}$$

During the optimization of particles in the range from −90° to 90°, the particle positions of all Q-dimensions must be limited to the ranges of particle positions regardless of whether they are initialized or updated. Because limiting the range of particles prevents them from moving to the wrong location, when the particle position is updated via Eq. (31), if the particle position exceeds the range, its position is adjusted to θ_{min} or θ_{max}. The second part of Eq. (30), $c_1 \boldsymbol{r}_1^h \times [\boldsymbol{pbest}_j^h - \boldsymbol{\theta}_j^h]$ is the impact of the historical best position of particles' own experiences on speed, which belongs to the self-cognition mode. The third part of Eq. (30), $c_2 \boldsymbol{r}_2^h \times [\boldsymbol{gbest}_g - \boldsymbol{\theta}_j^h]$, is the impact of the global historical best position on speed, which can be viewed as a social learning model. $c_1 \boldsymbol{r}_1^h$ and $c_2 \boldsymbol{r}_2^h$ represent the vectors formed by uniformly distributed random variables from 0 to 1 in the hth iteration and are the random acceleration terms of $\boldsymbol{pbest}_j^h = [pbest_{j,1}^h, pbest_{j,1}^h, \cdots, pbest_{j,Q}^h]$ and $\boldsymbol{gbest}_g = [gbest_{g,1}, gbest_{g,2}, \cdots, gbest_{g,Q}]$, respectively. The learning factors c_1 and c_2 will affect the acceleration of the particles, and their purpose is to push the particles to the optimal position. Generally, the values of c_1 and c_2 are set as 2 to let the average of $c_1 \boldsymbol{r}_1^h$ and $c_2 \boldsymbol{r}_2^h$ equal 1. The fitness value can be calculated through the fitness function to maximize the fitness function to find the DOA of the signal. After that, let the termination error be μ_2 and define the termination condition of the DOA search of the swarm intelligence algorithm to compare it with the previous fitness function value, and $|fitness(\boldsymbol{\theta}_j^{h-1}) - fitness(\boldsymbol{\theta}_j^h)| \leq \mu_2$. If the fitness function value accumulated 50 times is less than or equal to μ_2, it means that the performance of this algorithm is no longer changing and is converging, that is, the iteration is stopped and the termination condition is met. At this time, a set of global best fitness function values $fitness(\boldsymbol{\theta}_{gbest}) = fitness(\boldsymbol{\theta}_j^h)$ are obtained. A fitness value corresponds to a set of global best solutions $gbest_g$; otherwise, the iteration continues. $fitness(\boldsymbol{\theta}_j^h)$ and $fitness(\boldsymbol{\theta}_j^{h-1})$ represent the fitness function values of the jth swarm of particles in the hth and (h + 1)th iterations and

correspond to $\boldsymbol{\theta}_j^h = [\theta_{j,1}^h, \theta_{j,2}^h, \cdots, \theta_{j,Q}^h]$ and $\boldsymbol{\theta}_j^{h-1} = [\theta_{j,1}^{h-1}, \theta_{j,2}^{h-1}, \cdots, \theta_{j,Q}^{h-1}]$ respectively. Finally, the steps to implement the PSO search for DOA estimation are as follows:

Step 1: Set the maximum number of iterations h_{max}, the number of particles N_p, the initial position $\boldsymbol{\theta}_j^h$, and the initial velocity $\boldsymbol{v}_j^h$.

Step 2: Start the search using the initial position $\boldsymbol{\theta}_j^h$ and the velocity $\boldsymbol{v}_j^h$; the measurement and search for the global optimal solution are carried out using the maximizing fitness function (29). $\boldsymbol{pbest}_j^h$ and $\boldsymbol{gbest}_{\boldsymbol{g}}$ found by the PSO algorithm are resepectively the best individual and group positions in one iteration measured using Eq. (29).

Step 3: For the $\boldsymbol{pbest}_j^h$ and $\boldsymbol{gbest}_{\boldsymbol{g}}$ found by the algorithm at the hth iteration, the inertia weight w^h is updated according to Eq. (32), and the speed and position of each particle are updated according to Eqs. (30) and (31), respectively, for the next iteration.

Step 4: When the termination condition $|\, fitness(\boldsymbol{\theta}_j^{h-1}) - fitness(\boldsymbol{\theta}_j^h) \,| \le \mu_2$ has been satisfied and the number of comparisons accumulated over 50 times of the fitness function, stop the execution of the algorithm, and $\hat{\boldsymbol{\theta}} = \boldsymbol{gbest}_{\boldsymbol{g}}$ is the estimated DOA.

3.2 QPSO-based DOA estimator

In this subsection, we present a novel approach to DOA estimation based on PSO with the QPSO algorithm. Unlike the standard PSO algorithm,[13] which relies on particles and swarm's experiences, the proposed method (i.e., QPSO) employs a search trajectory that is designed to converge to the optimal solution. In the standard PSO algorithm, the particles follow the previously established trajectory and gradually reach the convergence state, resulting in the search space of each iteration of the particle being unable to cover the entire feasible space during the search process. Therefore, the accuracy of local searches is not optimal, and the convergence rate decreases as the search process progresses. To enhance the optimal search capability and convergence speed of particles within the feasible region and to overcome the limitations of the standard PSO algorithm, quantum concepts are integrated into the PSO algorithm.[15] In QPSO, each particle exhibits quantum behaviors during the search process. Consequently, only the particle's position vector and a control parameter are considered, which results in a higher convergence speed and an enhanced optimization ability. The QPSO algorithm represents a developed version of the PSO algorithm that does not require a velocity vector with fewer parameters and is easier to implement.

Assume that the Q-dimension of quantum space consists of N_p particles and the position of the jth particle is expressed as $\boldsymbol{\theta}_j = [\theta_{j,1}, \theta_{j,2}, \cdots, \theta_{j,Q}]$ and j = 1, 2, …, N_p. The particle passes through the historical best position and is denoted by $\boldsymbol{p}_j = [p_{j,1}, p_{j,2}, \cdots, p_{j,Q}]$. In quantum space, a particle's position after undergoing a random Monte Carlo measurement simulation is determined as follows:

$$\theta_{j,i} = p_{j,i} \pm \frac{L}{2} \cdot \ln\left(\frac{1}{u}\right), \;\; j = 1,2,\cdots,N_p, \;\; i = 1,2,\cdots,Q, \tag{33}$$

where u is a uniformly distributed random variable from 0 to 1 and $L = 2 \cdot \beta \cdot | p_{j,i} - \theta_{j,i} |$ is the value obtained from the particle's current position and its historical best position. Therefore, the updated equation for quantum PSO is

$$\theta_{j,i}^{h+1} = p_{j,i}^{h} \pm \beta | p_{j,i}^{h} - \theta_{j,i}^{h} \cdot \ln\left(\frac{1}{u}\right)|, \tag{34}$$

where h is the number of iterations of the algorithm and β is the contraction and expansion coefficient and the only parameter of the QPSO. It is generally defined to implement a linear decrease in the range between 1 and 0.5. To avoid premature convergence, we employed the average best position $mbest_i^h$ into the QPSO algorithm, which is given by

$$mbest_i^h = \frac{1}{N_p} \sum_{j=1}^{N_p} p_{j,i}^h, \ i = 1, 2, \cdots, Q, \tag{35}$$

where $mbest_i^h$ finds the average best position of N_p particles and solves the problem on the basis of dimensions of the variables. After introducing $mbest_i^h$, the individual update formula is

$$L = 2 \cdot \beta \cdot | mbest_i^h - \theta_{j,i}^h |, \tag{36}$$

$$\theta_{j,i}^{h+1} = p_{j,i}^h \pm \beta \cdot | mbest_{j,i}^h - \theta_{j,i}^h | \cdot \ln\left(\frac{1}{u}\right). \tag{37}$$

Therefore, the particle update equation of QPSO can be described as

$$p_{j,i}^h = \varphi \cdot p_{j,i}^h + (1 - \varphi) \cdot p_{g,i}, \tag{38}$$

$$\boldsymbol{mbest}^h = [mbest_1^h, mbest_2^h, \cdots, mbest_Q^h], \tag{39}$$

$$\boldsymbol{\theta}_j^{h+1} = \boldsymbol{p}_j^h \pm | \boldsymbol{mbest}^h - \boldsymbol{\theta}_j^h | \cdot \ln\left(\frac{1}{u}\right), \tag{40}$$

where φ is a random variable in the interval [0, 1]; other parameters are the same as those mentioned above. Finally, the steps to implement the QPSO searching to perform DOA estimation are as follows:

Step 1: Set the maximum number of iterations h_{max}, the number of particles N_p, and the initial position $\boldsymbol{\theta}_j^h$.

Step 2: Use the initial position $\theta_{j,i}^h$ to start searching and maximize the fitness function [Eq. (29)] to measure and search for the global best solution. $p_{j,i}^h$ and $p_{g,i}$ found by the QPSO algorithm are respectively the individual best position and the swarm best position of the next iteration measured using Eq. (29).

Step 3: Update the inertia weight w^h using Eq. (32) for $p_{j,i}^h$ and $p_{g,i}$ found by the algorithm in the hth iteration, and at this time, the range of inertia weight w^h values is defined as $[w_{min}, w_{max}] = [0.5, 1]$. According to Eqs. (38)–(40), the position of each particle is updated for the next iteration.

Step 4: If the termination condition $\left|fitness(\theta_j^{h-1}) - fitness(\theta_j^h)\right| \le \mu_2$ is met and the accumulated 50 times adaptive function value comparisons are achieved, then stop the execution of the algorithm. That is, $\hat{\boldsymbol{\theta}} = \boldsymbol{p}_g$ is the desired estimated DOA and $\boldsymbol{p}_g = [p_{g,1}, p_{g,2}, \cdots, p_{g,Q}]$.

4. Simulation Results

In this section, we provide computer simulation results to demonstrate the effectiveness of the PSO-based estimators (PSO-APA, PSO-HADPA, and PSO-HDAPA) and QPSO-based estimators (QPSO-APA, QPSO-HADPA, and QPSO-HDAPA) for DOA estimation. For comparison, the results of the conventional spectrum-searching-based APA, HADPA, and HDAPA are also provided.[19] In the HAD massive antenna system, all simulation environments of the DOA estimator employ the binary phase shift keying (BPSK) modulation method, and the average power of users is equal. We define $\mathrm{SNR} = 10\log_{10} E\{(y^b)^2\} / \sigma_v^2$ and the root mean square error $\mathrm{RMSE} = (1/\Pi Q)\sqrt{\sum_{\rho=1}^{\Pi}\sum_{i=1}^{Q}(\theta_i^\rho - \hat{\theta}_i^\rho)^2}$, where Π is the number of Monte Carlo trials. Suppose the number of the antenna deployment of the HAD massive antenna system N is 32. In each simulation, the results are obtained through $L = 200$ and $\Pi = 100$. The number of users $Q = 4$, and the impinging angle of signals $\theta = \{-45^\circ, -25^\circ, 10^\circ, 30^\circ\}$. If the searching grid size μ_1 is smaller and the estimation performances of the APA, HADPA, and HDAPA estimators improve, then the selection of the searching grid μ_1 is determined as $\mu_1 = 10^{-2}$. Relatively, the performances of all the PSO-based estimators will be improved as the termination error μ_2 becomes smaller. Therefore, the selection of the termination error μ_2 is $\mu_2 = 10^{-8}$. Table 1 illustrates the effective search parameter setting for the PSO and QPSO algorithms.

Figures 2 and 3 illustrate the selection of numbers of iterations and particles for the APA, HADPA, and HDAPA methods using the PSO- and QPSO-based search estimators, respectively. First, the general behaviors of the {PSO-APA, PSO-HADPA, PSO-HDAPA} and {QPSO-APA, QPSO-HADPA, and QPSO-HDAPA} estimators are examined. Assume that the variation ranges of SNR and the number of iterations h_{max} are $\mathrm{SNR} = [0\mathrm{dB}, 30\mathrm{dB}]$ and $h_{max} = [10, 310]$, respectively; then, set the number of particles $N_p = 200$. Figures 2(a) and 3(a) illustrate the RMSE performances of the {PSO-APA, PSO-HADPA} and {QPSO-APA, QPSO-HADPA} estimators, respectively, as functions of the numbers of iterations and particles. Figures 2(b) and 3(b) present the RMSE performances of PSO-HDAPA and QPSO-HDAPA, respectively, as functions of the

Table 1
Effective search parameter settings.

Algorithm	Parameters
PSO	$w_{max} = 0.9$, $w_{min} = 0.4$, $c_1 = c_2 = 2$
QPSO	$\beta_{max} = 0.9$, $\beta_{min} = 0.4$

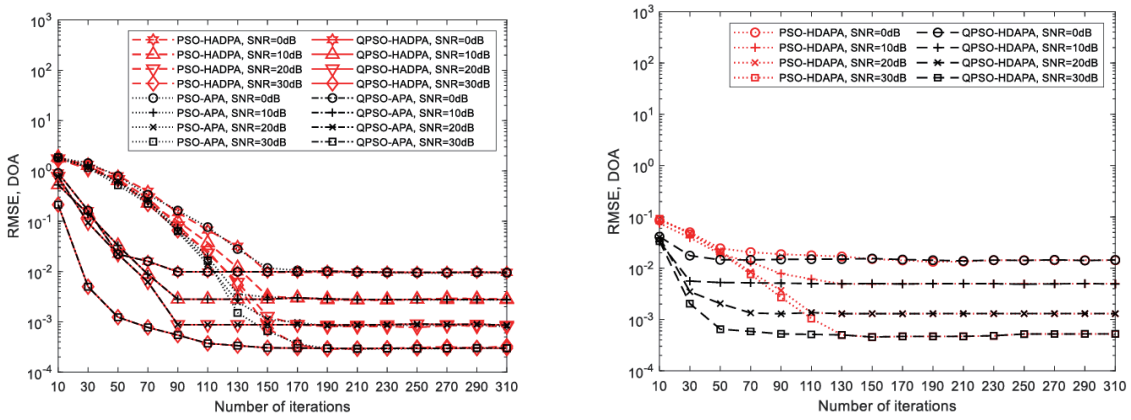

(a) (b)

Fig. 2. (Color online) RMSE of DOA estimation versus number of iterations. (a) PSO-APA, PSO-HADPA, QPSO-APA, and QPSO-HADPA. (b) PSO-HDAPA and QPSO-HDAPA.

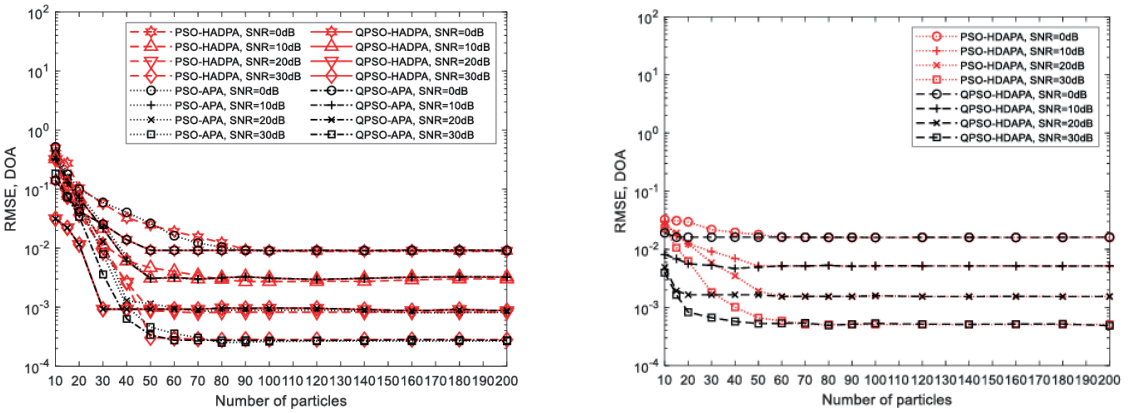

(a) (b)

Fig. 3. (Color online) RMSE of DOA estimation versus number of particles. (a) PSO-APA, PSO-HADPA, QPSO-APA, and QPSO-HADPA. (b) PSO-HDAPA and QPSO-HDAPA.

numbers of iterations and particles. The results indicate that the RMSE performance of {PSO-APA, PSO-HADPA} can achieve convergence when the number of particles is 90 and the number of iterations is 190. Similarly, the MSE performance of {QPSO-APA, QPSO-HADPA} can converge when the number of particles is 70 and the number of iterations is 150. The results of PSO-HDAPA indicate that when the number of particles is 70 and the number of iterations is 150, the estimation performance converges, which results in the PSO-HDAPA having good estimation in both search and convergence. However, the RMSE performance of QPSO-HDAPA converges when the number of particles is 50 and the number of iterations is 90. It is observed that the fundamental performances of the PSO-based and QPSO-based estimators are contingent upon the numbers of iterations and particles selected. The probability of identifying the optimal solution can be enhanced by incorporating a greater number of particles. Nevertheless, the

necessity of evaluating a greater number of particles entails a proportional increase in computational load. One of the key parameters in the swarm intelligence search algorithm is the size of the population. The QPSO differs from the PSO in several respects. First, the update [Eq. (34)] of QPSO ensures that particles appear in the entire-dimensional search space at each iteration, whereas in PSO, particles can only fly in a bounded space at each iteration. Second, the QPSO employs a different approach to the PSO in that it does not require the calculation of the inertia weight, which is a significant advantage.

In the DOA estimation, the desired impinging angles from signal sources can be estimated by APA, HADPA, and HDAPA. However, these methods may not have better estimation performance when dealing with noisy signals. Furthermore, the performance of angle estimation accuracy is contingent upon the size of the search grid μ_1, and thus, it is less advantageous than the other methods in terms of the capabilities that can be resolved. Conversely, angle estimation methods based on swarm intelligence algorithms demonstrate excellent performance and are relatively cost-effective in terms of the capabilities they offer. The swarm intelligent algorithm employs a simulation of the living habits of animals in nature to identify targets within a solution space. Each particle represents the optimal solution within the solution space. The movement of particles will gradually shift from the global area to the local area in proximity to the target. This implies that all particles will move towards the target, thereby increasing the degrees of freedom (resolution capabilities of DOA estimates) in searching for the targets. Figure 4 illustrates the RMSE of DOA estimation versus SNR. As SNR increases, the estimation performance of all estimators improves. The proposed methods offer satisfactory estimation performance and, at the same time, exhibit a reduced computational complexity.

Note that the basic performances of the PSO-based estimators depend on the numbers of iterations and particles selected. More particles can increase the success probability of searching for the best solution. However, more particles require more evaluation operations, resulting in a higher computational load. The size of the population is a crucial factor in PSO-based search algorithms. When the population size is insufficient, it often indicates that optimal solutions are more challenging to identify if the particles do not adequately encompass the entire search space, which could result in the omission of the global optimum.

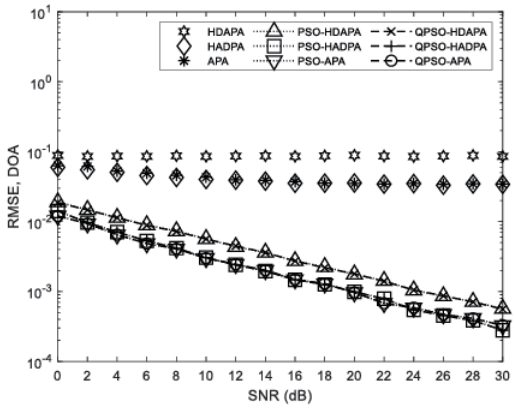

Fig. 4. RMSE of DOA estimation accuracy versus SNR.

Table 2
Results of calculated fitness function analysis.

DOA estimators	Number of particles	Number of iterations	Computational complexity
PSO-APA	90	190	17100
PSO-HADPA	90	190	17100
PSO-HDAPA	70	150	10500
QPSO-APA	70	150	10500
QPSO-HADPA	70	150	10500
QPSO-HDAPA	50	90	4500

The size of the population is one of the important parameters in the PSO-based search algorithms. If the population size is very small, it is harder to find the best solution if the particles do not cover the entire search space. This could mean that the best solution is missed. To calculate the fitness function and achieve a relatively stable estimation performance, the required number of iterations, the number of particles, and computational complexity (defined as the product of the numbers of iterations and particles) for the PSO and QPSO searching estimators are presented in Table 2. For the computational complexity of spectrum-searching-based DOA estimators (APA, HADPA, and HDAPA), defined as the searching space of angle $\theta = [-90^\circ,\ 90^\circ]$, if the search grid size μ_1 is 1°, 0.1°, or 0.01°, the number of searches is 181, 1801, or 18001, respectively. To achieve superior DOA estimation accuracy, the smaller searching grid size of spectrum-searching-based DOA estimators results in significant increases in the number of mass searches and computational cost. Table 2 indicates that the number of searches of all PSO and QPSO algorithms are less than 18001. In essence, the proposed QPSO-based methods reduce the substantial computational load by reducing the product of the numbers of particles and iterations, while maintaining relatively optimal estimation performance.

5. Conclusions and Future Work

In this paper, we presented an efficient DOA sensing method based on PA on the antenna sensor array of mIoT, which employs a PSO search for an HAD massive MIMO receiving array. Conventional APA, HADPA, and HDAPA will require exponentially more complex multiplications for spectrum search, resulting in a significant calculation load. The proposed QPSO-HDAPA estimator has the potential to significantly reduce the required number of iterations and the number of particles, thereby considerably reducing the computational complexity of spectrum search. Nevertheless, the simulation results have demonstrated that the proposed PSO-based and QPSO-based estimators can achieve high resolution performance while also being able to estimate the DOA.

In the future, the applications of smart devices with mIoT techniques will be around people living in the extended application domains of mIoT techniques, such as smart cities, healthcare, disaster rescue, energy transformation, smart farming, cooperative intelligent transport systems, and environmental monitoring. For the wireless connections between mIoT sensors, the DOA estimation accuracy of the hybrid array affects the performance of network access capability directly. As future work, we plan to optimize the parameters of the proposed DOA estimators.

Moreover, additional heuristic optimization algorithms, such as Henry gas solubility optimization and fuzzy theory, will be explored to reduce hardware cost and energy consumption. Furthermore, 2D DOA sensing will be performed on the antenna sensor array in mIoT networks to accurately localize distributed mIoT devices, achieving low cost, low energy consumption, high localization precision, real-time signal transmission, and environmental adaptability. In the next stage, we will extend our studies on 2D DOA sensing in mIoT networks using the proposed methods to address the localization challenges of distributed mIoT devices in massive MIMO systems. Specifically, both the azimuth and elevation angles of impinging electromagnetic wave signals will be estimated.

References

1 M. Groth, M. Rzymowski, K. Nyka, and L. Kulas: IEEE Access **8** (2020) 91435. https://doi.org/10.1109/ACCESS.2020.2994364
2 X. Zhan, Z. Sun, F. Shu, Y. Chen, X. Cheng, Y. Wu, Q. Zhang, Y. Li, P. Zhang, and J. Zhao: Chin. J. Electron. **33** (2024) 175. https://doi.org/10.23919/cje.2022.00.112
3 S. A. Khwandah, J. P. Cosmas, P. I. Lazaridis, Z. D. Zaharis, and I. P. Chochliouros: Wireless Pers. Commun. **120** (2021) 2101. https://doi.org/10.1007/s11277-021-08550-9
4 M. A. Islam, G. C. Alexandropoulos, and B. Smida: Proc. 2022 IEEE Communications Conf. (IEEE, 2022) 4673. https://doi.org/10.1109/ICC45855.2022.9838368
5 F. Shu, Y. Qin, T. Liu, L. Gui, Y. Zhang, J. Li, and Z. Han: IEEE Trans. Commun. **66** (2018) 2487. https://doi.org/10.1109/TCOMM.2018.2805803
6 Z. Li, R. Pu, Y. Xia, W. Pei, and D. P. Mandic: IEEE Trans. Signal Process. **69** (2021) 4257. https://doi.org/10.1109/TSP.2021.3096431
7 M. M. Gunjal and A. B. Raj: Proc. 2020 5th Communication and Electronics Systems Conf. (IEEE, 2020) 249. https://doi.org/10.1109/ICCES48766.2020.9137982
8 S. Keerthi, K. Ashwini, and M. Vijaykumar: Int. J. Comput. Appl. Technol. **115** (2015) 8. https://doi.org/10.5120/20145-2273
9 X. Jia and G. Lu: IEEE Antennas Wirel. Propag. Lett. **18** (2019) 1581. https://doi.org/10.1109/LAWP.2019.2924247
10 P. Babbar, S. Saxena, S. Mishra, and A. Rajawat: 2021 2nd Global Conf. Advancement in Technology (IEEE, 2021) 1. https://doi.org/10.1109/GCAT52182.2021.9587552
11 C.-L. Meng, S.-W. Chen, and A.-C. Chang: Wireless Pers. Commun. **81** (2015) 343. https://doi.org/10.1007/s11277-014-2132-1
12 J.-C. Hung: Processes **8** (2020) 1429. https://doi.org/10.3390/pr8111429
13 J. Kennedy and R. Eberhart: Proc. ICNN'95 Neural Networks Conf. 4 (IEEE, 1995) 1942. https://doi.org/10.1109/ICNN.1995.488968
14 M. Xi, J. Sun, and W. Xu: Appl. Math. Comput. **205** (2008) 751. https://doi.org/10.1016/j.amc.2008.05.135
15 J. Sun, C.-H. Lai, and X.-J. Wu: Particle Swarm Optimisation: Classical and Quantum Perspectives (Crc Press, New York, 2016) Chap. 4.
16 C. E. Garcia, M. R. Camana, and I. Koo: IEEE Trans. Green Commun. Networking **7** (2022) 649. https://doi.org/10.1109/TGCN.2022.3219111
17 J. Sun, W. Xu, and B. Feng: Proc. 2004 Cybernetics and Intelligent Systems Conf. 1 (IEEE, 2004) 111. https://doi.org/10.1109/ICCIS.2004.1460396
18 Z. Jiankui, H. Zishu, and L. Benyong: 2006 CIE Int. Conf. Radar (2006) 1. https://doi.org/10.1109/ICR.2006.343252
19 I. Ahmed, H. Khammari, A. Shahid, A. Musa, K. S. Kim, E. D. Poorter, and I. Moerman: IEEE Commun. Surv. Tutorials **20** (2018) 3060. https://doi.org/10.1109/COMST.2018.2843719

About the Authors

Tsui-Ping Chang received her B.S. and M.S. degrees from the National Yunlin University of Science and Technology, Yunlin, Taiwan, in 1998 and 2000 respectively, and Ph.D. degree from the Department of Computer Science and Engineering at National Chung-Hsing University, Taichung, Taiwan, in 2009. She joined the Department of Computer Science and Information Engineering, National Taichung University of Science and Technology as an associate professor in 2019. Her research interests include web data mining, cloud computing, and artificial intelligence.

Chao-Li Meng was born in Taichung Taiwan R.O.C, 1974. He received his B.S degree from Dayeh University, Changhua, Taiwan, in 1996, and M.S. degree from the Department of Information Technology Ling Tung University, Taichung Taiwan, in 2011, and Ph.D. degree from the Program of Electrical and Communications Engineering, Feng Chia University, Taichung, in 2017. He is currently working as a program manager at the AIoT Research Center, Feng Chia University, Taichung, Taiwan. His research interests include adaptive array, multiuser detection, OFDM, 5G wireless systems, and mobile location for wireless communications.